RESEARCH ARTICLE

Botany

The vessel wall thickness–vessel diameter relationship across woody angiosperms

Alberto Echeverría ⬤ | Emilio Petrone-Mendoza ⬤ | Alí Segovia-Rivas |
Víctor A. Figueroa-Abundiz | Mark E. Olson ⬤

Instituto de Biología, Universidad Nacional
Autónoma de México, Tercer Circuito s/n de
Ciudad Universitaria, Ciudad de México, 04510,
México

Correspondence
Mark E. Olson, Instituto de Biología, Universidad
Nacional Autónoma de México, Tercer Circuito
s/n de Ciudad Universitaria, Ciudad de México,
04510, México.
Email: molson@ib.unam.mx

Abstract

Premise: Comparative anatomy is necessary to identify the extremes of combinations of functionally relevant structural traits, to ensure that physiological data cover xylem anatomical diversity adequately, and thus achieve a global understanding of xylem structure–function relations. A key trait relationship is that between xylem vessel diameter and wall thickness of both the single vessel and the double vessel+adjacent imperforate tracheary element (ITE).

Methods: We compiled a comparative data set with 1093 samples, 858 species, 350 genera, 86 families, and 33 orders. We used broken linear regression and an algorithm to explore changes in parameter values from linear regressions using subsets of the data set to identify a threshold, at 90-μm vessel diameter, in the wall thickness–diameter relationship.

Results: Below 90 μm diameter for vessels, virtually any wall thickness could be associated with virtually any diameter. Below this threshold, selection is free to favor a very wide array of combinations, such as very thick walls and narrow vessels in ITE-free herbs, or very thin-walled, wide vessels in evergreen dryland pioneers. Above 90 μm, there was a moderate positive relationship.

Conclusions: Our analysis shows that the space of vessel wall thickness–diameter combinations is very wide, with selection apparently eliminating individuals with vessel walls "too thin" for their diameter. Most importantly, our survey revealed poorly studied plant hydraulic syndromes (functionally significant trait combinations). These data suggest that the full span of trait combinations, and thus the minimal set of hydraulic syndromes requiring study to span woody plant functional diversity adequately, remains to be documented.

KEYWORDS

allometry, angiosperms, broken linear regression, morphological space, natural selection, plant hydraulics, Sherwin Carlquist, thickness-to-span ratio, vessel diameter, vessel wall thickness, xylem anatomy

In their efforts to construct an adequate picture of xylem function, xylem physiologists and comparative xylem anatomists need to work together closely (Sterck et al., 2012; Steppe et al., 2015). One way that comparative anatomy can guide physiology studies is by revealing global patterns of covariation in traits of functional interest (Janssen et al., 2020) and highlighting the extremes in these trends. Without such studies, it is difficult to know whether or not experimental studies have adequately covered the diversity of xylem structural strategies and hydraulic syndromes (functionally significant trait combinations) spanned by plants. A key trait relationship in the secondary xylem is the functional connection between the thickness of conduit walls and conduit diameter (Hacke and Sperry, 2001; Larter et al., 2015).

Alberto Echeverria and Emilio Petrone-Mendoza authors share first authorship.

Despite clear reasons to regard the wall thickness–conduit diameter relationship as functionally important, there is little empirical information regarding any broad relationship across vessel-bearing plants. This gap is important because the current lack of information makes it difficult to distinguish between two possibilities. One possibility is that there is a strong relationship between wall thickness and vessel diameter. For a given wall thickness, wider tubes are more prone to buckling, so selection would be expected to favor wall thicknesses that are sufficient to resist severe deformation or even implosion (Hacke et al., 2001; Donaldson, 2002; Karam, 2005; Jacobsen et al., 2005; Pratt et al., 2007; Spatz and Niklas, 2013). Across species, the thickness of intervessel pit membranes predicts vulnerability to embolism well (Li et al., 2016; Kaack et al., 2021), and across species wider vessels often have predictably thinner intervessel pit membranes (Lens et al., 2011; Scholz et al., 2013b), so, to the extent that vessel diameter might be associated with embolism vulnerability, these data provide additional reasons to expect a wall thickness-diameter relationship. Even gas flow across the cell wall itself is likely lower across thicker walls (Sorz and Hietz, 2006; Venturas et al., 2017). Along these lines, plants with vessels with walls that are thicker for a given diameter are more resistant to embolism (Hacke and Sperry 2001; Jacobsen et al., 2005, 2007; Pratt et al., 2007; Lens et al., 2011; Guet et al., 2015; Thonglim et al., 2020). So, while there are multiple potential reasons to expect that vessel wall thickness is significant in embolism resistance, all point to thicker walls being associated with greater resistance. If, all else being equal, wider vessels are more vulnerable to buckling and to embolism, it would be unsurprising to find that across species vessel diameter predicts wall thickness (Blackman et al., 2018; Pfautsch et al., 2018). Accordingly, a positive relationship between wall thickness and vessel diameter is often assumed in models of xylem function (Mencuccini et al., 2007; Hölttä et al., 2011).

Another possibility is that there is a very wide range of wall thicknesses that can be functional for a given vessel diameter, depending on the conditions of natural selection across species. Consistent with this possibility are observations that species in drylands have thicker walls for a given conduit diameter than those in moist areas (Baas et al., 1983; Hacke et al., 2001; Olson et al., 2003; Pratt et al., 2007; Nardini et al., 2012) as well as studies that fail to find a relationship between wall thickness and vessel diameter, either across the members of a clade from different habitats, or across the members of a community (Cochard et al., 2008; Lens et al., 2011; Chen et al., 2020). The negative pressures in conduits vary widely across species and even across conduits in the same stem (Bouda et al., 2019), suggesting that the conditions of selection can vary greatly for the same vessel diameter. These observations seem to indicate that a wide range of wall thicknesses are possible for a given conduit diameter. There are thus reasons to expect both that

conduit diameter should and should not strongly predict wall thickness. Distinguishing empirically between these possibilities is therefore a priority for efforts such as understanding how plant hydraulic systems are shaped by selection as well as for modeling conduit carbon costs.

Mapping the space of vessel wall thickness–diameter relations across species is important for identifying the ways that developmental possibility interacts with selection in producing the observed range of wall thickness–diameter combinations (cf. Leslie and Losada 2019). The range of developmentally possible conduit wall thickness–diameter relationships defines the space of possibilities that selection can favor (Olson, 2012). If wall thickness and diameter are so correlated developmentally that some combinations are not possible, then these combinations cannot be observed even if they would be favored by selection (Figure 1A) (Olson, 2019). On the other hand, the range of developmentally possible combinations could be wide, with selection favoring a very wide range of wall thickness–conduit diameter combinations across habits and habitats, such that a predictable wall thickness–conduit diameter relationship is not observed across species (Figure 1B). Another possibility is that the range of developmentally possible combinations is wide, but that selection tends to favor proportionality, such that a wall thickness–conduit diameter relationship is observed across species (Figure 1C). Investigating these scenarios requires sampling that covers as much of the vessel-bearing angiosperm phylogeny as possible, from both self- and non-self-supporting habits. If there is a relationship between wall thickness and vessel diameter, then sampling as widely as possible would identify its generality. If selection is free to favor a wide range of wall thickness–conduit diameter relationships such that there is no predictable relationship, then this space of possibilities should emerge most clearly when sampling across as wide a range as possible of lineages, habits, and habitats. Therefore, we aim to test here whether there is a relationship between vessel wall thickness and vessel diameter and whether this relationship varies across species with different perforation plate types, imperforate tracheary element types, and self-versus non-self-supporting status, in the single vessel wall thickness and the double vessel+adjacent imperforate tracheary element wall.

To provide wall thickness–vessel diameter data from a very wide range of non-monocot angiosperms, we compiled data from the comparative studies of Sherwin Carlquist spanning over six decades, from 1957 to 2018 (a list of studies cited is given in the data set, available from the TRY plant trait database). The wide range covered in these studies allowed us to test for the relationship between vessel wall thickness and vessel diameter from 858 species from 82 families covering a very wide array of climates and life forms. Drawing on the works of a single author helped eliminate heterogeneity in ways that traits were measured (e.g., external or internal vessel diameter (Carlquist, 2001; Scholz et al., 2013a) or classifications of imperforate tracheary elements (Carlquist, 1986; Rosell et al., 2007;
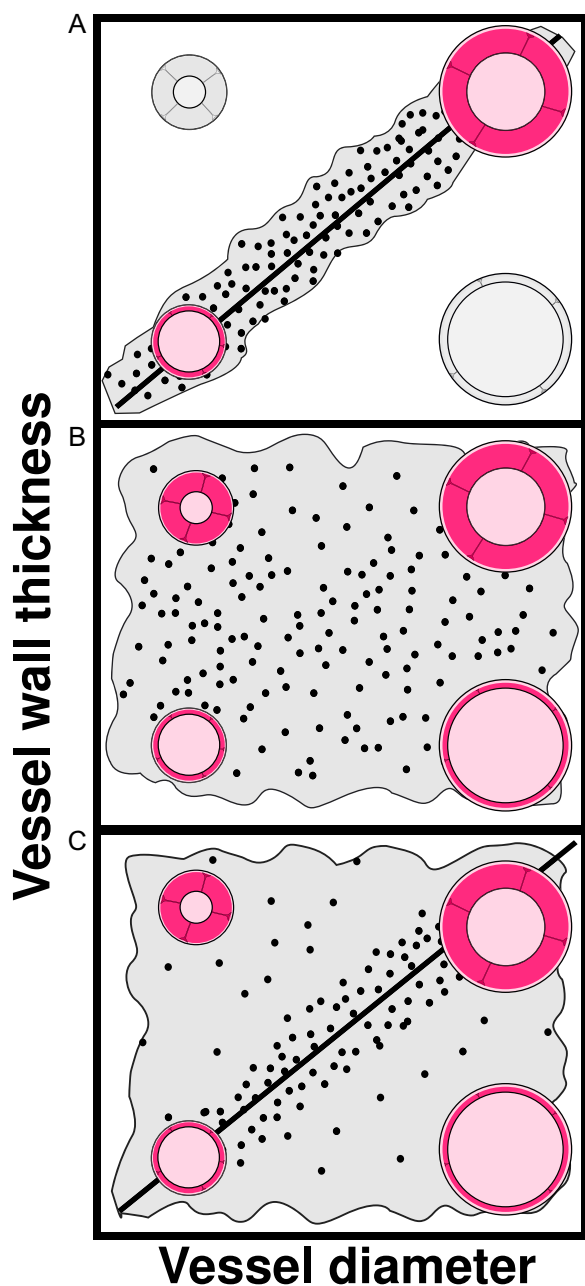
FIGURE 1 Possible relationships between vessel wall thickness and vessel diameter. The gray fields represent the areas where data points fall and thus the field of manifestly developmentally possible thickness–diameter combinations. (A) One possibility is that vessel wall thickness and vessel diameter covary strongly for (unknown) developmental reasons, such that a strong positive relationship is observed (red variants). Because of this developmental covariation, narrow vessels with thick walls and wide vessels with thin walls (gray variants) cannot be observed, even if they would be favored by selection. (B) Another possibility is that vessel wall thickness and diameter can vary independently of one another in development. Selection is therefore free to favor such a wide range of combinations, depending on selective context, that a wide space of combinations is observed and no relationship emerges. (C) Another possibility is that a very wide range of combinations is developmentally possible, as in B, but that selection tends to favor a positive wall thickness–diameter relationship, with most data falling along a scaling line. Possible but uncommon variants (the data points above and below the main scaling line) are observed only in rare situations.

Olson et al., 2020), providing comparability across a large data set.

MATERIALS AND METHODS

Data set assembly

Examining the vessel wall thickness–vessel diameter relationship across the flowering plants required wall thickness–vessel diameter data from as wide a range as possible of phylogenetic lineages, climates, and plant habits. We compiled the data from Sherwin Carlquist's wood anatomy publications given that they provide comparable data from a very wide range of angiosperm diversity. Compiling the data set consisted of two main steps. The first involved capturing the data for the variables of interest as they appear in the original publications. The second involved creating curated variables suitable for statistical analysis. We assigned species to orders based on quartil Angiosperm Phylogeny Group IV (Chase et al., 2016), while family, genus, species, and authority were based mainly on World Flora Online (www.worldfloraonline.org). In a few cases, species were not listed there, so we used the International Plant Names Index (ipni.org) or Tropicos (tropicos.org). Additionally, we checked binomials using the R package Taxonstand (Cayuela et al., 2021) to identify spelling errors or synonyms. The name *Faujasia blixana* appears in quotes in the original publication, and we were unable to locate it in any index or publication. We therefore denote it as *Faujasia* sp. in the data set. We recorded in the data set the publication from which we took the data as well as collection numbers, so that even when the name has changed, a given sample can be traced to the original study. In general, vessel diameter was measured as lumen diameter as a chord between the widest and narrowest diameters on transections under the light microscope, or as the diameter visible in macerations in species in which distinguishing vessels from conductive imperforate tracheary elements was difficult in transection. In some cases, such as *Seguieria americana* (Carlquist, 2000), vasicentric tracheids were so abundant and overlapped so extensively in diameter with vessels that measuring vessel grouping accurately from transverse sections was impossible, and grouping is not reported in these species. Vessel grouping is not reported for only 6.5% samples of the dataset (71 of the 1093). Wall thickness was usually measured at a point judged to be "representative", excluding the often-thicker areas in the corners of angular vessels. The data are from secondary xylem.

We recorded data as given in the publications, and in generating the curated variables for statistical analysis, we made various decisions. In the case of vessel diameter, means were usually given per sample, and these were used directly for analysis. In five cases, however, ranges or diameters for wide and narrow vessels were given. In these cases, we calculated means using the values given. In the

case of *Fuchsia pachyrrhiza* P.E.Berry & B.A.Stein, *Stein et al. 4066*, vessel diameter was reported as 0.41 μm, but measuring the vessels based on the scale given in the photograph in the original publication, 41 μm seems more likely, and we used this value. We followed similar procedures for vessel wall thickness and imperforate tracheary element wall thickness and diameter. In the case of *Cneorum pulverulentum* Vent., *Carlquist 2350*, vessel wall thickness was reported in the original publication as being 14 μm. This value was so far outside the range of other wall thickness reported for all other members of the genus (2.4–3.4 μm) that it seemed safest to exclude this sample from analysis as likely representing a printer's error. We included both the raw data and the curated variables in the dataset, so that all of the decisions we took can be consulted.

We also made analogous decisions for categorical variables. For perforation plate type, in most cases a single type is reported. In a few cases, however, different perforation plate types were mixed in the same sample. We coded the state for analysis based on the type reported as being preponderant in a given sample. Perforation plate types in virtually all cases were either simple (with no cell wall material traversing the plate) or scalariform (with bars forming many narrow perforations making up the perforation plate). Our curated variable had just two states, simple or scalariform. In the case of imperforate tracheary element (ITE) type we followed Carlquist's classification, which includes true tracheids, fiber-tracheids, and libriform fibers (Carlquist, 1986; Rosell et al., 2007; Olson et al., 2020). Co-occurrence of ITE types was sometimes reported. In these cases, for statistical analysis, we coded the ITE type reported as being most frequent.

We also included analyses aimed at taking into account evidence that perforation plate and ITE type could be associated with variation in the wall thickness–diameter relationship. Our dataset allowed us to test the ability of mean vessel diameter to predict vessel wall thickness across species as well as the relationship between diameter and the double wall made up by the vessel wall plus the adjacent imperforate tracheary element wall ("double wall thickness"). Vessels are adhered to their adjacent cells via the middle lamella. This means that stress imposed by negative pressure is likely resisted not just by the vessel wall but propagated to adjacent cells, and some data suggest that the double wall thickness does contribute to resisting embolism (Hacke et al., 2001; Hacke and Sperry, 2001; Jacobsen et al., 2005; Pittermann et al., 2006; Chen et al., 2020; Janssen et al., 2020; though see Levionnois et al., 2021). The double wall thickness that is the object of selection in the context of negative pressures within vessels necessarily differs between species with solitary vessels and those with grouped vessels. Species with solitary vessels usually have true tracheids, which conduct water, and therefore the relevant double wall thickness that resists negative pressures is the vessel+ITE double wall thickness. In species with grouped vessels, it is the vessel-vessel double wall that is expected to be strongly subject to selection, because it is this

wall that resists deformation when one vessel embolizes adjacent to a functional one (Hacke and Sperry, 2001; Jacobsen et al., 2005). For species with mean vessel groupings lower than 1.5, we calculated the double wall thickness as the sum of the vessel wall+ITE wall thicknesses, while for species with vessel grouping higher than 1.5, we calculated the double wall as the vessel wall thickness multiplied by two.

Along these lines, potentially affecting the vessel wall thickness–diameter association are differences in mean wall thickness between species with simple versus scalariform perforation plates or different types of imperforate tracheary elements. Vessels with scalariform perforation plates are known for having relatively thin walls (Frost, 1930; Carlquist, 2001) and, because they are largely confined to moist habitats, are likely on average subject to much less negative xylem pressures than species with simple perforation plates. We therefore examined the possibility that given vessel diameter, species with scalariform perforation plates have thinner vessel walls than those with simple perforation plates. Imperforate tracheary elements (ITEs, referred to as "fibers" in some classification systems (Wheeler et al., 1989), see table of Olson et al. (2020) comparing classification systems) are the main support cells in woody plants, and in the classification we follow here are made up of three types (Carlquist, 1984, 1986; Rosell et al., 2007; Olson, 2020; Olson et al., 2020). Tracheids (Carlquist's "true tracheids") have abundant pits with borders that are wide relative to the pit aperture. Libriform fibers have sparse pits with no borders, and fiber-tracheids have sparse pits with narrow borders. Tracheids are conductive, and libriform fibers and fiber-tracheids are nonconductive (Sano et al., 2011; Carlquist, 2017; Olson, 2020). To examine these issues, we tested for differences in wall thickness between ITE types given vessel diameter, which might be expected given their differences in structure. For example, true tracheids always have fully bordered pits, and a very thin wall would leave scant space for a pit aperture and pit chamber. As a result, true tracheids could be expected to have thicker walls than libriform fibers with their simple pits. Because, as described above, ITE wall thickness affects the fiber+vessel double wall thickness that in turn likely affects embolism resistance, there are reasons to think that ITE type could affect the relationship between the vessel wall, or double wall, and vessel diameter.

Our data set included a total of 33 orders, 86 families, 350 genera, 858 species, and 1093 samples. Most species were represented by a single sample (81%), but some species were represented by multiple collections. The species with the largest numbers of samples were *Turpinia occidentalis* (7 samples) and *Moringa drouhardii* (6 samples). The values of each sample were used for analyses because there were relatively few multiple samples in the data set, precluding use of mixed models, and because in any case we were interested in documenting whether or not there is a relationship between vessel wall thickness and vessel diameter, and if there is it should be observed across samples within-species as well as across.

Statistical analyses: finding the threshold value above which wall thickness is predicted by diameter

Preliminary inspection showed a clear trend characterized by an apparent change in slope in the wall thickness–vessel diameter relationship. This change suggested that over the range of vessel diameter covering the narrower vessels, vessel diameter did not predict wall thickness. In wider-diameter vessels, diameter did appear to predict wall thickness. We used two approaches to explore quantitatively whether there is a statistically significant change in the wall thickness–vessel diameter relationship. The first approach was broken linear regression. For this procedure, we used a model comparing the hypothesis of a changepoint in the data against the null hypothesis of no changepoint, using the R package lm.br (Adams, 2014). The second approach consisted of ordering the data from the narrowest vessel diameter to the widest vessel diameter and partitioning the data (total $N = 1093$) into four subsets, each with the same number of observations ($N = 273$). The first partition contained the narrowest vessel diameter values, and the last partition contained the widest vessel diameters. For each partition, we fitted 100 thickness–diameter models based on 100 measurements, sampling without replacement, saving the coefficients of determination, slope, and P-values from each model. If there were a relationship between vessel diameter and vessel wall thickness above but not below a certain vessel diameter, then our approach should reveal higher coefficients of determination and slope values for the models in the partitions containing wider vessel diameters. As we discuss in more detail in the Results section, these two procedures coincided in indicating a change in the vessel wall thickness–vessel diameter relationship at 90 μm. We therefore separated the data set at this threshold and fit separate models predicting wall thickness based on vessel diameter for the sets above and below this value.

Statistical analyses: single and double wall thickness, perforation plate type, and imperforate tracheary element types

Having identified the threshold value above which vessel diameter has some ability to predict wall thickness, and below which there is no relationship, we then proceeded to explore various key factors that potentially could influence the wall thickness–vessel diameter relationship. Our main focus was on the possible differences between the ability of vessel diameter to predict single versus double wall thicknesses. Because wall thickness likely varies across different types of imperforate tracheary elements that participate in making up the vessel+ITE double wall, it was necessary to investigate the effect that variation in ITE type might have on wall thickness. Because true tracheids are commonly associated with scalariform perforation plates, it was also necessary to take perforation plate type

into account as well. We fitted linear models predicting double wall thickness based on vessel diameter, perforation plate type, and/or imperforate tracheary element type, along with their interactions. Given the low coefficients of determination of these models with a single categorical variable, it is not surprising that those with two categorical variables (perforation plate type and ITE type) and their interaction terms also explained little of the variance in wall thickness. Because of their low fits, and because models with several predictor variables and interaction terms are very difficult to interpret biologically, only models with one categorical variable and vessel diameter are provided in Table 1. We fit all linear models using the lm function in R (v.4.0.3, R Core Team, 2020). For these models, we included all of the species in the data set.

We also explored the differences in wall thicknesses of vessels, ITEs, and double walls between species with different perforation plate types and imperforate tracheary element types classified as conductive (true tracheids) and nonconductive (libriform fibers) independently of vessel diameter, using t-tests. For these t-tests, we excluded species with fiber-tracheids. As we explain in the Discussion section, our results suggest that some species are likely miscategorized, with some species with true tracheids currently categorized as having fiber-tracheids. To ensure that our inferences truly reflect the differences between conductive and nonconductive ITEs, we included only species categorized as having true tracheids, which are almost certainly all conductive, and libriform fibers, which are virtually certainly all non-conductive (Sano et al., 2011).

Scalariform perforation plates are commonly associated with true tracheids (Olson et al., 2020), potentially confounding the relationship between perforation plate type, vessel diameter, and wall thickness. To take this possibility into account, we tested for an association between ITE type and perforation plate type by constructing a 2×2 contingency table between species with simple versus scalariform perforation plates on one hand versus nonconductive ITEs (libriform fibers and fiber-tracheids) and conductive ones (tracheids) on the other (for discussion of the ITE classification used and its importance for elucidation of function, see Carlquist, 1984, 1986; Rosell et al., 2007; Sano et al., 2011; Olson, 2020; Olson et al., 2020). We used χ^2 tests to test for an association between ITE type and perforation plate type and standardized residuals from the χ^2 tests to quantify the degree of relationship between categorical associations.

Statistical analyses: ecological diversity

We then explored the breadth of ecological diversity spanned by the sampled species. First, to characterize species with the most extreme combinations of the wall thickness–vessel diameter space below 90 μm, we first used a subset of the species below the first and above the third quartiles of vessel diameter. For each subset of the vessel diameter quartiles, we

TABLE 1 Linear models predicting vessel wall thickness based on vessel diameter, above and below the 90 µm threshold

Model	N	R^2	Model ANOVA	Slope equality test	Intercept equality test	Slope (CI)	Intercept (CI)
Models for vessel diameters below 90 µm							
Vessel wall thickness ~ Conduit diameter	866	0.001	$F_{1,865}=2.49$	—	—	0.04 (−0.01, 0.8)	0.34 (0.26, 0.41) $P < 0.001$
Vessel wall thickness ~ Conduit diameter + perforation plate type + Conduit diameter*perforation plate type	866	0.08	$F_{3,862}=24.65$ $P<0.001$	$P<0.001$	—	Scalariform = 0.42(0.28, 0.55); Simple = 0.03 (−0.02, 0.08)	Scalariform = −0.39(−0.62, −0.16); Simple = 0.36 (0.29, 0.44)
Vessel wall thickness ~ Conduit diameter + ITE conductiveness + Conduit diameter*ITE conductiveness	849	0.05	$F_{3,845}=15.94$ $P<0.001$	$P=0.01$	$P=0.01$	Conductive = 0.18 (0.07, 0.30); Nonconductive = 0.02 (−0.02, 0.07)	Conductive = 0.03 (−0.16, 0.22); Nonconductive = 0.37 (0.29, 0.45)
Double wall thickness ~ Conduit diameter	782	0.04	$F_{1,780}=32.25$ $P<0.001$	—	—	0.13 (0.09, 0.18) $P<0.001$	0.52 (0.44, 0.59) $P<0.001$
Double wall thickness ~ Conduit diameter*perforation plate type + Conduit diameter*perforation plate type	782	0.11	$F_{3,778}=33.91$ $P<0.001$	$P<0.001$	—	Scalariform = 0.63 (0.48, 0.78); Simple = −0.05 (0.01, 0.10)	Scalariform = −0.29 (−0.55, −0.03); Simple = 0.63 (0.56, 0.71)
Double wall thickness ~ Conduit diameter + ITE conductiveness + Conduit diameter*ITE conductiveness	782	0.05	$F_{3,778}=15.41$ $P<0.001$	$P<0.001$	—	Conductive = 0.34 (0.22, 0.46); Nonconductive = 0.10 (−0.05, 0.15)	Conductive = 0.19 (−0.01, 0.39); Nonconductive = 0.57 (0.49, 0.65)
Models for vessel diameters above 90 µm							
Vessel wall thickness ~ Conduit diameter	224	**0.42**	$F_{1,222}=158.7$ $P<0.001$	—	—	0.81 (0.69, 0.94)	−1.18 (−1.45, −0.91)
Vessel wall thickness ~ Conduit diameter + perforation plate type + Conduit diameter*perforation plate type	224	**0.47**	$F_{2,221}=100.7$ $P<0.001$	$P=0.132$	$P<0.001$	Scalariform = 0.73 (−0.59, 0.84); Simple = 0.73 (0.60, 0.85)	Scalariform = −1.08 (−1.34, 0.82); Simple = −0.97 (−1.24, −0.70)
Vessel wall thickness ~ Conduit diameter + ITE conductiveness + Conduit diameter*ITE conductiveness	224	**0.42**	$F_{2,221}=80.83$ $P<0.001$	$P=0.312$	$P=0.147$	0.80 (0.67, 0.93)	−1.18 (−1.45, −0.91)
Double wall thickness ~ Conduit diameter	209	**0.28**	$F_{1,207}=79.08$ $P<0.001$	—	—	0.53 (0.42, 0.65)	−0.27 (−0.53, −0.02)
Double wall thickness ~ Conduit diameter + perforation plate type + Conduit diameter*perforation plate type	209	**0.29**	$F_{2,205}=29.47$ $P<0.001$	$P=0.008$	$P<0.001$	Scalariform = −0.06 (−0.51, 0.39); Simple = 0.58 (0.45, 0.70)	Scalariform = 0.95 (0.02, 1.88); Simple = −0.37 (−0.64, −0.09)
Double wall thickness ~ Conduit diameter + ITE conductiveness + Conduit diameter*ITE conductiveness	209	**0.29**	$F_{2,206}=42.98$ $P<0.001$	0.66	0.022	Conductive = 0.55 (0.43, 0.67); Nonconductive = 0.55 (0.43, 0.66)	Conductive = −0.26 (−0.51, −0.01); Nonconductive = −0.31 (−0.56, −0.06)

Notes: ITE conductiveness = conductive versus nonconductive imperforate tracheary elements (conductive = true tracheids; nonconductive = libriform fibers and fiber-tracheids), VD = vessel diameter, PP = perforation plate type, Int = interaction term. Coefficient of determination for multiple models is adjusted R^2.
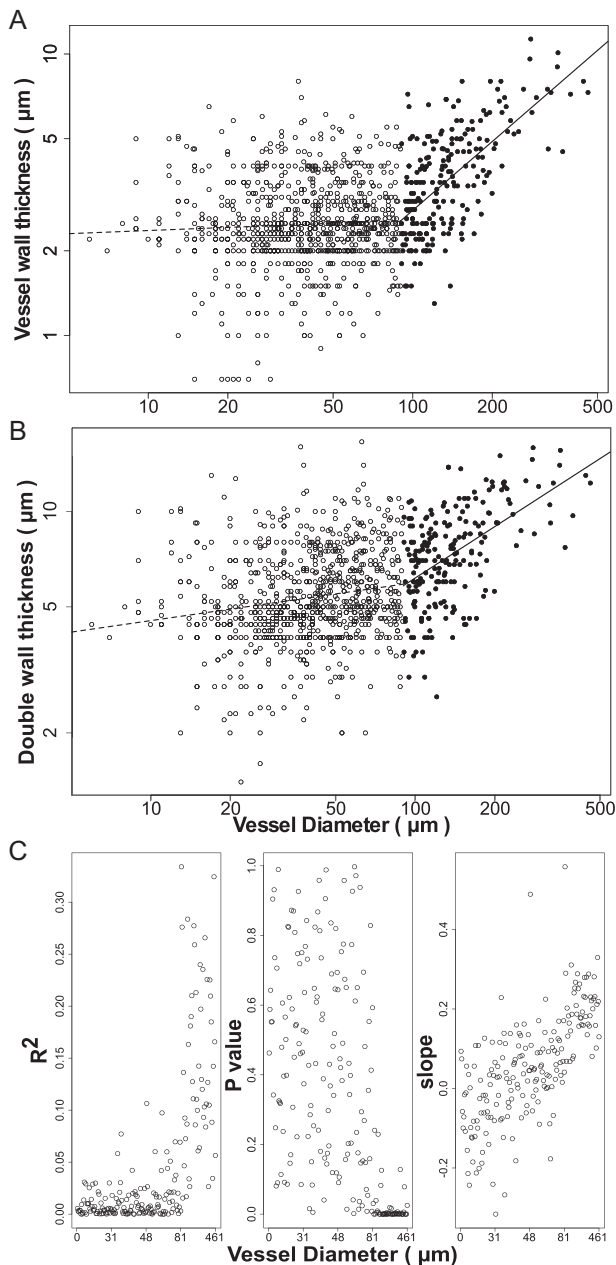
FIGURE 2 No vessel wall thickness–vessel diameter relationship below 90 μm vessel diameter, weak relationship above. (A) Broken linear regression showed that in the vessel wall thickness–vessel diameter relationship, there is a threshold at 90 μm (CI: 81–102 μm) vessel diameter. Below 90 μm, the relationship is weak ($R^2 = 0.01$), and above this threshold, the relationship has a moderately high coefficient of determination ($R^2 = 0.42$). (B) Double wall thickness follows a similar trend, with no relationship with conduit diameter below the threshold and a moderate relationship above ($R^2 = 0.27$). (C) We then fit models predicting wall thickness based on vessel diameter for different vessel diameter subsets of our data set (0–31 μm, 31–48 μm, 48–81 μm, 81–461 μm). Each point represents a different model. The thickness–diameter models fit with narrow vessels (the first three partitions) had very low R^2 values, high (nonsignificant) P-values, and low slopes (indicating no relationship). In contrast, in the last partition (which included the widest vessels), the R^2 were much higher, the P-values were significant, and the slopes were higher. Together, these analyses show that there is no relationship between vessel wall thickness and vessel diameter below 90 μm, and a moderate positive relationship above. Model fits are shown in Table 1.

selected the 15 samples with thinnest and thickest walls in the first and third quartiles of vessel wall thickness, resulting in four extreme combinations of vessel wall thickness–vessel diameter. To obtain spatial distribution and ecological information of the sampled species, we used the R package BIEN (Maitner et al., 2018). To retrieve the coordinates where the studied species grow, we used the BIEN_occurrence_species function. We then harvested climate information from the Worldclim database using the raster and sp packages (Hijmans et al., 2021; Pebesma et al., 2021). We also used the kgc library to retrieve Köppen climate classifications for each georeferenced species (Kottek et al., 2006; Bryant et al., 2017). To assemble functional trait data such as "growth form woodiness" (woody, herbaceous, or "variable"), wood density, and evergreen vs deciduous, we used the BIEN_trait_species function. We also collected information for the evergreen vs deciduous trait from the TRY database (Kattge et al., 2020). We used these data to see whether the sampled species span a wide range of the climates in which woody plants grow globally, and whether the species with extreme combinations of vessel wall thickness and vessel diameter fall uniformly throughout climate space or instead show distinctive ecological preferences. We performed all analyses in R.

RESULTS

Mean vessel diameter was 64.43 μm, spanning a very wide range, from 6 to 461 μm, while mean ITE diameter was 24.87 μm, ranging from 7 to 62 μm. Mean vessel wall thickness was 2.9 μm, ranging from 0.70 to 11.30 μm, while mean ITE wall thickness was 3.31, ranging from 0.40 to 14 μm.

Our results showed that below a threshold value, there was no relationship between either the single or double wall thickness and vessel diameter, but above this threshold, which represented 21% of the data, there was a moderately strong relationship (Figure 2, Table 1). Broken linear regression revealed a change of slope in the relationship between vessel wall thickness and vessel diameter at 90 μm (CI: 81–102 μm) (Figure 2A). The relationship between double wall thickness and vessel diameter followed a similar pattern because of the lack of a predictable relationship between ITE wall thickness and vessel diameter (not shown), with no relationship between double wall thickness and vessel diameter below the threshold, and a weaker relationship than that between single wall thickness and vessel diameter above the threshold ($R^2 = 0.27$, Figure 2B). Congruent with the results of the broken linear regression, the results of the linear models fit with random subsets of species with vessel diameters ranging from 6 to 31 μm showed low R^2 values (ranging from 6.87×10^{-6} to 0.04) and nonsignificant P-values (mean value of P: 0.49), contrasting with models from the subset containing vessel diameters from 81 to 461 μm, which had higher R^2 values (ranging from 0.05 to 0.51, mean value 0.14) and significant P-values (mean value of $P < 0.02$) (Figure 2C). Above the 90 μm

threshold, wall thickness scaled with vessel diameter with a slope of 0.81 (95% CI 0.69, 0.94; Table 1). All of these results point to there being a very wide range of wall thickness–diameter relations below the threshold and a more restricted pattern above.

In the entire data set, 11% of the species were non-self-supporting; above the 90 μm threshold, 29% of the species were non-self-supporting and plants with vessel diameters above 230 μm (461 μm maximum value) were exclusively non-self-supporting. Because non-self-supporting plants were disproportionately represented above the 90 μm threshold, it seemed possible that there could be different wall thickness–vessel diameter relationships between self- and non-self-supporting plants. Rejecting this notion, we found similar changes in vessel wall thickness–vessel diameter slopes when self- and non-self-supporting plants were examined separately.

Because vessel wall thickness was not predicted by vessel diameter below the 90 μm threshold, we examined the influence of perforation plate type and imperforate tracheary element type on vessel wall thickness without including vessel diameter for plants below the threshold (90 μm vessel diameter; Figure 3A–F) and fitted linear models to plants above it (Table 1; Appendix S1).

Plants with scalariform perforation plates tended to have thinner vessel walls ($t = -5.71$, df = 100.69, $P < 0.001$, Figure 3A) but thicker ITE walls ($t = 5.62$, df = 103.28, $P < 0.001$, Figure 3B). Similarly, plants with conductive ITEs tended to have thinner vessel walls than plants with nonconductive ITEs ($t = -5.34$, df = 213.44, $P < 0.001$, Figure 3D), but thicker ITE walls ($t = 5.47$, df = 223, $P < 0.001$, Figure 3E). Double wall thickness was similar in plants with scalariform and simple perforation plates ($t = 1.4$, df = 91.71, $P = 0.16$, Figure 3C), and among plants with conductive and nonconductive ITEs ($t = 1.09$, df = 199.51, $P = 0.28$, Figure 3F). Estimation of the double wall thickness as the sum of ITE and vessel wall thicknesses gave similar results. Thinner single vessel wall thickness in plants with scalariform plates contrasted with their double wall thickness, reflecting their preferential association with conductive ITEs.

We confirmed that scalariform perforation plates are preferentially associated with conductive ITEs with a contingency table (Table 2). Plants with scalariform perforation plates tended to have conductive ITEs (true tracheids), while plants with simple perforation plates tended to have nonconductive ITEs (libriform fibers or fiber-tracheids) (Table 2, $\chi^2 = 126.6$, df = 1, $P < 0.0001$). Association between perforation plate type and ITE type and the wide range of vessel wall thickness–vessel diameter combinations below the 90 μm threshold suggested varying ecological strategies, which we explored by identifying the species occupying the extreme regions of the morphospace. Species with extreme combinations of single and double wall thickness and vessel diameter are given for the four quadrants of the wall thickness–vessel diameter space below 90 μm in Table 3. These quadrants correspond to species with thick walls and narrow vessels, thin walls and narrow
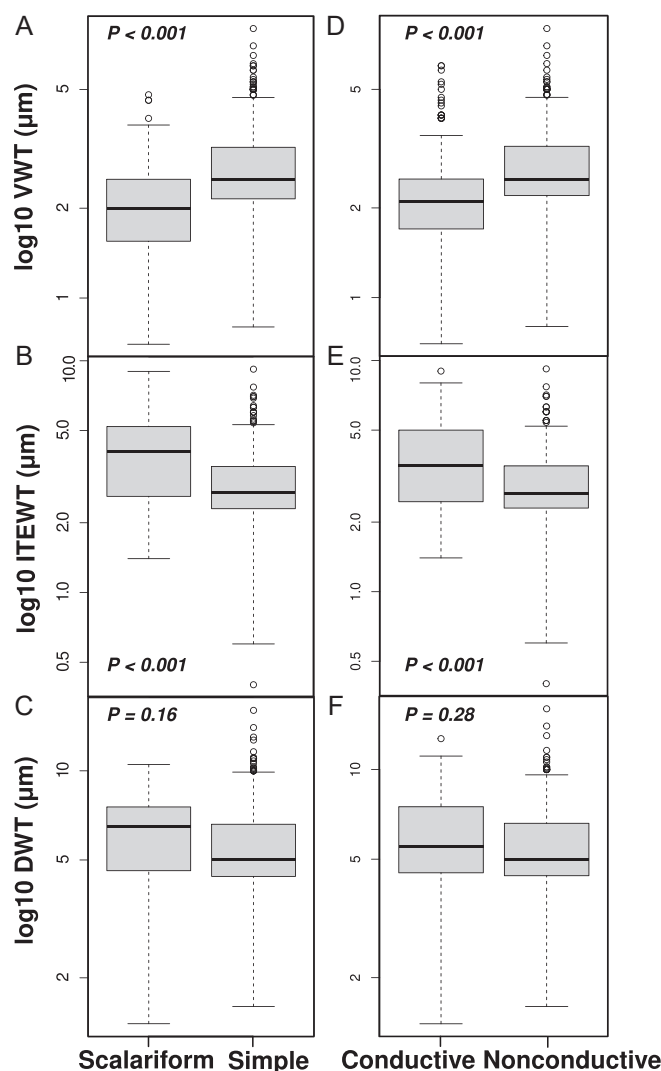

FIGURE 3 Evidence consistent with the double wall being a target of selection. (A) Species with scalariform perforation plates had significantly thinner single vessel wall thickness (VWT) than species with simple plates. (B) In contrast, species with scalariform perforation plates had significantly greater ITE wall thickness (ITEWT) than species with simple plates. (C) These differences even out when examining double wall thickness (DWT), with species with scalariform perforation plates and simple perforation plates having statistically indistinguishable double wall thicknesses. (D) Similarly, species with conductive ground tissue ITEs (true tracheids) had thinner vessel walls than species with (nonconductive) libriform fibers. (E) Species with (conductive) true tracheids had thicker ITE walls than species with libriform fibers, consistent with the notion that conductive status requires thicker ITE cell walls on average (F) Again, species with conductive and nonconductive ITEs have similar thicknesses of the double cell wall, consistent with the expectation that selection should favor similar double wall thicknesses at interfaces between conductive cells, even in the context of great variation in individual cell wall thickness.

vessels, thick walls and wide vessels, and thin walls and wide vessels. Details regarding ITE and perforation plate type are given in Appendix S2, based on single vessel wall thickness, and in Appendix S3, based on double (vessel+ITE) wall thickness. The species occupying each quadrant suggest functionally significant trait combinations, and we tested

Perforation plate type	ITE type		Total
	Nonconductive (libriform fibers + fiber-tracheids)	Conductive (true tracheids)	
Scalariform	100 (155.04) **–11.35**	90 (34.96) **11.35**	190
Simple	778 (722.96) **11.35**	108 (163.04) **–11.35**	886
Total	878	198	1076

TABLE 2 Contingency table showing preferential association between scalariform perforation plates and true tracheids and between simple perforation plates and nonconductive ITEs (libriform fibers and fiber-tracheids).

Notes: The association between perforation plate type and ITE type can be seen in the differences between observed frequencies and expected frequencies shown in parentheses and by the values of the standardized residuals derived from a χ^2 test that are greater than 2 shown in bold, reflecting the association between perforation plate type and ITE type.

whether these combinations were related to climate and other functional traits.

We recovered climate information for 670 species (78%) of the 858 total. These data showed that the sampled species cover essentially all of woody plant climate space and that species with extreme combinations of vessel wall thickness and vessel diameter occupy distinct areas of climate space (Appendix S4). Plotting the frequency of occurrence in our data of Köppen climate type, which were available for 665 species, revealed a pattern very similar to the distribution of species worldwide, with most being found in tropical habitats and very few coming from the cold climates of species-poor high latitudes (Appendix S5A). Plots of the distribution of Köppen climates across species with extreme combinations of vessel wall thickness and vessel diameter (Appendix S5B) underscore the ecological distinctness, discussed in more detail below, of the species falling in these quadrants of vessel wall thickness–diameter space. Appendix S6 shows the distribution of herbaceous/woody and evergreen/deciduous status across the vessel wall thickness–vessel diameter relationship. Herbaceous species below the threshold represent 17% of observations recovered from the BIEN traits database, contrasting with just 3.2% of observations recovered for herbaceous species above the threshold. Woody plants occupied 93.6% of observations above the threshold and 81% of observations below it. Most plants above the threshold were evergreen (87.3%, with 55 observations, versus 12.7% deciduous, with 8 observations). Most species were evergreen below the threshold (71%, with 164 observations), though the percentage of deciduous species was higher than above it (29%, with 66 observations). Wood density data were not available for most of the species with extreme values of vessel wall thickness–vessel diameter residuals (Appendix S7), but the data that were available did follow the expected patterns (e.g., the single species with very thick vessel walls and narrow vessels had, as expected, relatively high wood density; Appendix S8A). The expected patterns were also observed across the entire data set, with wood density scaling negatively with vessel diameter; larger plants have lower wood density and wider vessels (Appendix S8B) (Olson et al., 2021; Fajardo, 2022). Wood density showed a tendency to be higher in species with thicker double walls (Appendix S8C), and, as expected, a stronger tendency to be higher in species with higher thickness-to-span ratios, either calculated using vessel wall thickness × 2 (Appendix S8D) or the double vessel+ITE wall (Appendix S8E).

DISCUSSION

Our results suggest that over a wide range of vessel diameter, selection is free to favor a comparably wide range of wall thicknesses (Figure 4A), but that very wide vessels with thin walls (the gray variant in Figure 4B) are always selected against. Below the threshold of 90 μm vessel diameter, the space of possible vessel wall thickness–vessel diameter combinations corresponds to our Figure 1B (Table 1, Figure 2C). In Figure 1B, the space of functionally favored combinations is sufficiently wide that no relationship between wall thickness and vessel diameter is observed and practically any combination of wall thickness–vessel diameter can be favored by selection. We detected a remarkable amount of biological signal in this pattern; examining the extremes of the vessel wall thickness–diameter relationship in this wide space below 90 μm vessel diameter identified trait combinations that have been studied little or not at all experimentally, and we highlight some of these below. We first examine the likely causes of the moderate tendency for vessel diameter to predict wall thickness above 90 μm vessel diameter.

Above 90 μm, selection eliminates vessels that have walls that are "too thin" or "too thick"

With regard to the "very thin walls-very wide vessels" portion at lower right in Figure 4A, there are at least three possibilities for explaining this empty space, the third of which seems most likely. One possibility is that the current data set, which covers a very wide span of phylogenetic lineages, habits, and habitats (Appendix S4), happens to exclude a significant portion of plant morphological and functional diversity, and that portion happens to be the one occupying the "very thin walls-very wide vessels" part of morphological space. That this empty space is the result of sheer sampling bias seems very unlikely. First, because vessel diameter scales predictably with stem length (Olson et al., 2021), the species in this area are necessarily either tall trees or long lianas. Furthermore, to fall in this quadrant, they need to have very thin walls. We have never observed, and are not aware of any studies documenting, large dicot trees or long lianas with extremely thin vessel walls. As a result, it seems very unlikely that the "very thin walls, very wide vessels" quadrant is unoccupied because of a lack of

TABLE 3 Ecological relationships of the four extreme combinations in the relationship between vessel wall thickness and vessel diameter.

Quadrant	Habitat	Species
Thick walls, narrow vessels (upper left)	Drylands	*Emorya suaveolens*
		Krameria secundiflora
		Krameria sonorae
		Malesherbia linearifolia
		Montinia caryophyllacea
		Phlox diffusa
		Stilbe albiflora
	Saline drylands	*Azima tetracantha*
		Limonium commune
		Salvadora persica
		Wilsonia humilis
	Moist temperate, herbaceous species with vessels embedded in a parenchyma background	*Helleborus viridis*
		Other cases not in the 15 most extreme but within the most extreme 28%:
		Calycera sympaganthera
		Dianthus caryophyllus
		Eremogone macradenia
		Misodendrum quadrifolium
		Silene fruticoides
Thin walls, narrow vessels (lower left)	Moist habitat shrubs or subshrubs	*Ceratiola ericoides*
		Hydrastis canadensis
		Empetrum eamesii sub sp. *eamesii*
		Empetrum nigrum sub sp. *hermaphroditum*
		Empetrum nigrum
		Empetrum rubrum
		Xanthorhiza simplicissima
	Seasonally dry shrubs	*Argyroxiphium kauense*
		Argyroxiphium sandwicense
		Buddleja stachyoides
		Buddleja colvilei
		Buddleja americana
		Dorystaechas hastata
		Morella quercifolia
		Origanum majorana
		Salvia dorrii
		Schiedea lydgatei
Thick walls, wide vessels (upper right)	Moist, often cool, forests, fiber-tracheids unless specified	*Ascarina diffusa*
		Ascarina solmsiana
		Ascarina swamyana
		Ascarina philippinensis

(Continues)

T A B L E 3   (Continued)

Quadrant	Habitat	Species
		Ascarina rubricaulis
		Daphniphyllum pentandrum (true tracheids)
		Degeneria roseiflora
		Espadaea amoena
		Myoporum tenuifolium
	Warm drylands, true tracheids	*Convolvulus floridus*
		Convolvulus scoparius
		Dicraspidia donnell-smithii
	Tropical, nonconductive ITEs	*Coccoloba longifolia*
		Corynocarpus dissimilis
		Meliosma cuneifolia
		Meliosma macrophylla
		Moringa rivae
		Nothocestrum breviflorum
		Nothocestrum latifolium
		Nothocestrum longifolium
		Sanchezia decora
		Sanchezia williamsii
Thin walls, wide vessels (lower right)	Moist forest, often tropical highland	*Begonia peruviana*
		Euscaphis japonica
		Hedyosmum brenesii
		Morella salicifolia
		Myrica nagi
		Myrica microcarpa
		Myrica rubra
		Staphylea colchica
		Tovaria pendula
		Turpinia occidentalis
	Often evergreen, often pioneer, low wood density	*Cestrum nocturnum*
		Duboisia myoporoides
		Eriodictyon californicum
		Hyptidendron arboreum
		Hyptis emoryi
		Hyptis mutabilis
		Martynia annua (annual)
		Nicotiana glauca
		Nicotiana tomentosa
		Presliophytum incanum
		Solanum gayanum
		Solanum rugosum
		Wigandia urens

adequate sampling. The second possibility is that, as in Figure 1A, the space of developmental possibility is, for unknown reasons, limited in such a way that only wall thicknesses that follow the 0.81 proportionality (Table 1) can be produced in plant development. Sometimes, morphologies are not observed because they are not possible to produce in development (Olson, 2012, 2019). For example, because a given volume of wood can be occupied by the cell walls that

contribute mechanical stiffness or the cell lumina that provide space for storage, there are no woods that simultaneously maximize mechanical stiffness and storage, even though selection would presumably favor such a combination if it were possible (Pratt and Jacobsen, 2017). So, one possibility is that the "walls too thin" area of wall thickness–vessel diameter space is empty because plants simply cannot produce very thin walls on very wide vessels for developmental reasons. This possibility seems clearly false. The cell walls of fusiform cambial initials are very thin (Larson, 1994; Chaffey et al., 2002). Vessel elements and ITEs are derived from these cells, so during maturation they traverse the space from thin to thick walls. Moreover, mutants exist with exceptionally thin mature tracheary element walls (Ranocha et al., 2010). Data such as these show that plants can indeed produce in development tracheary elements with extremely thin walls. This observation means that the absence of these in mature xylem cannot be explained by developmental impossibility. As a result, the third possibility is the most likely. The large space below the line strongly suggests that above a certain vessel diameter threshold, selection eliminates variants with walls that are "too thin", likely because they do not resist deformation either under flexion of the stem or under negative pressure within vessels. This possibility is supported by the observation that conduits with walls that are abnormally thin due to mutation or pathology tend to collapse under negative pressure (Turner and Somerville, 1997; Donaldson, 2002).

The space above the line (the upper variants in Figure 4B, C) is also developmentally accessible, certainly with respect to double wall thickness, as demonstrated by the species that occupy, albeit sparsely,
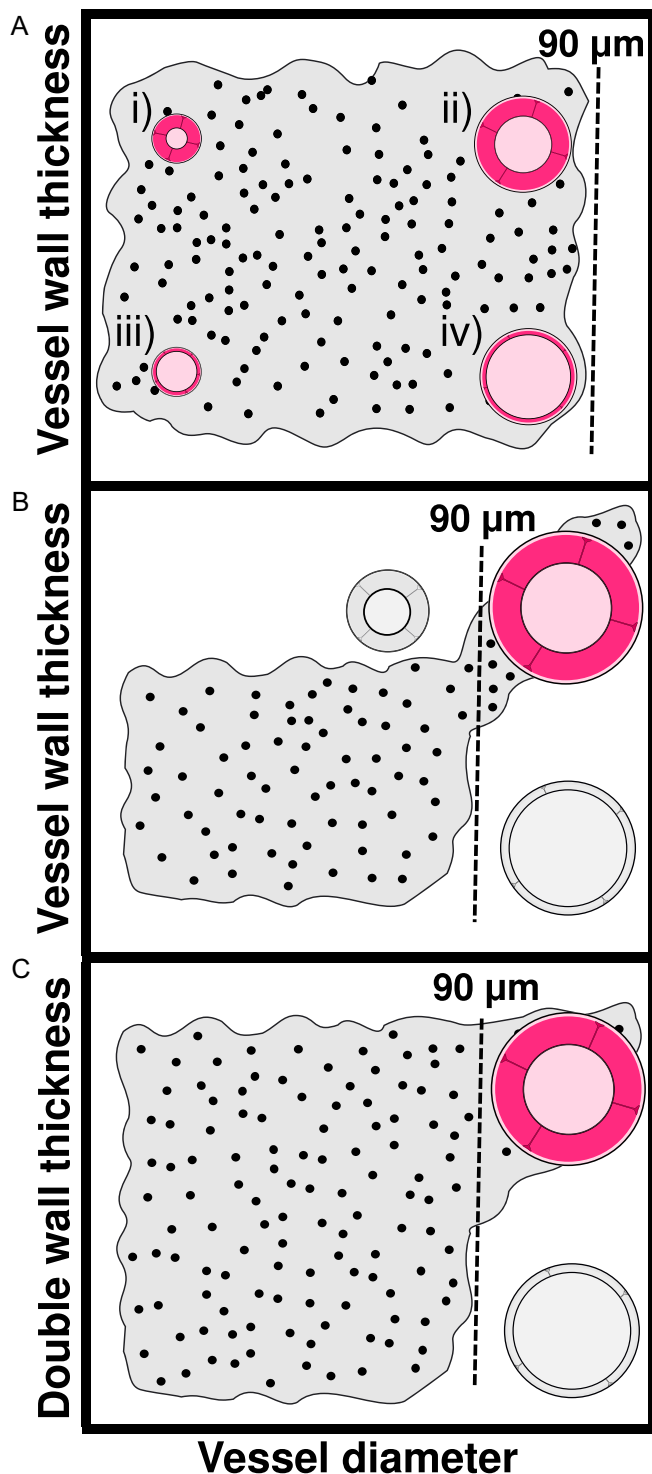

FIGURE 4 Selection favors a wide array of wall thickness–diameter relationships below the 90 μm diameter threshold and eliminates wide vessels with thin walls above. (A) Below 90 μm, a wide array combinations of vessel diameter and vessel wall thickness were observed, and the extremes in this space reveal understudied hydraulic syndromes. In the (i) upper left quadrant are species with narrow vessels and thick walls (dry, often saline environments and mesic herbs with vessels embedded in a parenchyma background). In the (ii) upper right quadrant are species with wide vessels and thick walls, mostly species with tracheids or fiber-tracheids. In the (iii) lower left quadrant are species with narrow vessels and thin walls, including subshrubs from moist environments as well as soft-leaved dryland species. At (iv) lower right are species with wide vessels and thin walls, which included evergreen dryland pioneer species. (B) With regard to the relationship between vessel wall thickness (single, not double wall), above the threshold, most species fell along a positive scaling line, with some species falling above the line, suggesting that these variants are indeed developmentally possible, if not favored in most situations. Below the line, species with very wide vessels and very thin walls were not observed. Because vessel walls pass through thin stages during development, presumably such variants are possible but not favored by selection. Below the threshold, species with wall thicknesses comparable to the thickest observed above the threshold were not observed, represented by the gray variant below the threshold. (C) With regard to the double wall thickness, the maximum wall thicknesses observed were similar above and below the threshold, indicating that these combinations are all developmentally possible. This wide space of developmental possibilities makes it likely that selection is free to favor the wall thickness–vessel diameter combination that is favored in a given situation.

this portion of the graph in Figure 2B. The space above the line in Figure 4B thus most plausibly corresponds to the situation in Figure 1C, in which selection tends to favor a predictable relationship within a space of very wide developmental possibility. The sparse occupation above the scaling line is almost certainly due to excessive carbon cost, and we are aware of no alternative hypothesis plausibly accounting for why plants do not routinely produce cell walls that are much thicker than those commonly observed. This interspecific pattern is consistent with the following causal scenario. Given variants within a population, those with similar

FIGURE 5 Relationship between perforation plate type and imperforate tracheary element (ITE) type and their respective wall thicknesses. (A) Vessels with simple perforation plates were more commonly associated with nonconductive cells (fiber-tracheids and libriform fibers, Table 2). (B) Vessels with scalariform perforation plates were most commonly associated with conductive ITEs (true tracheids). (C) Species with vessels with simple perforation plates had thicker single vessel walls (VWT) than species with scalariform perforation plates (D). However, with regard to double wall thickness (DWT; vessel+ITE wall thickness [ITEWT], or 2 × VWT), species with scalariform perforation plates had similar double walls as species with simple plates (Figure 3C, F).

performance (e.g., similar conductance) for a lower carbon cost will always be favored (Mencuccini et al., 2007; Hölttä et al., 2011; Koçillari et al., 2021). Vessel walls that are "too thick" for a given performance will therefore be uncommon, hence the sparse occupation of the area above the scaling line.

The double wall thickness as a target of selection

There is evidence that, in general, negative pressures in vessels are resisted not just by single vessel walls but by the double walls formed by vessels plus their adjacent cells (Hacke and Sperry, 2001; Jacobsen et al., 2005). From this point of view, the wall thickness that is expected to be favored by selection in the context of a given vessel diameter is the double wall, and our data provide observations consistent with this expectation. One observation consistent with this hypothesis is that species that lacked ITEs had exceptionally thick single vessel walls given vessel diameter. In species such as *Helleborus viridis* (described in the following subsection), there are no ITEs to which to transfer the mechanical loads imposed by negative pressures inside vessels (Carlquist, 1995). As a result, the single vessel wall must resist these loads, and so selection appears to achieve the favored wall thickness by the single wall alone.

Another observation is that, across the entire data set, Figure 3A shows that, while species with scalariform perforation plates have significantly thinner vessel walls than those with simple plates, they have significantly thicker ITE walls, with the result that species with simple and scalariform perforation plates have similar double wall thicknesses (Figures 3C, 5). Because of the way we calculated the double wall thickness, this result is likely to reflect selection on wall thickness at interfaces between conductive cells. When vessels were mostly solitary (<1.5 vessels/group), we calculated the double wall thickness as the vessel–ITE interface. When vessels were mostly grouped (>1.5 vessels/group), we calculated the double wall thickness as the vessel–vessel interface. In this way, we ensured that we were comparing conductive cell–conductive cell interfaces. Given that scalariform perforation plates tend to be associated with (conductive) true tracheids (Table 2), it could be that thicker walls are favored in conductive ITEs because, e.g., thicker walls better resist deformation in the event of embolization of conduits adjacent to functional ones, which leads to a great pressure differential across the embolized-functional double wall (Hacke and Sperry, 2001). Accordingly, species with conductive ITEs (true tracheids) had significantly thinner vessel walls (Figure 3D), and significantly thicker ITE walls than those with nonconductive ITEs (libriform fibers) (Figure 3E). If it is true that the double wall thickness resists mechanical loads under negative
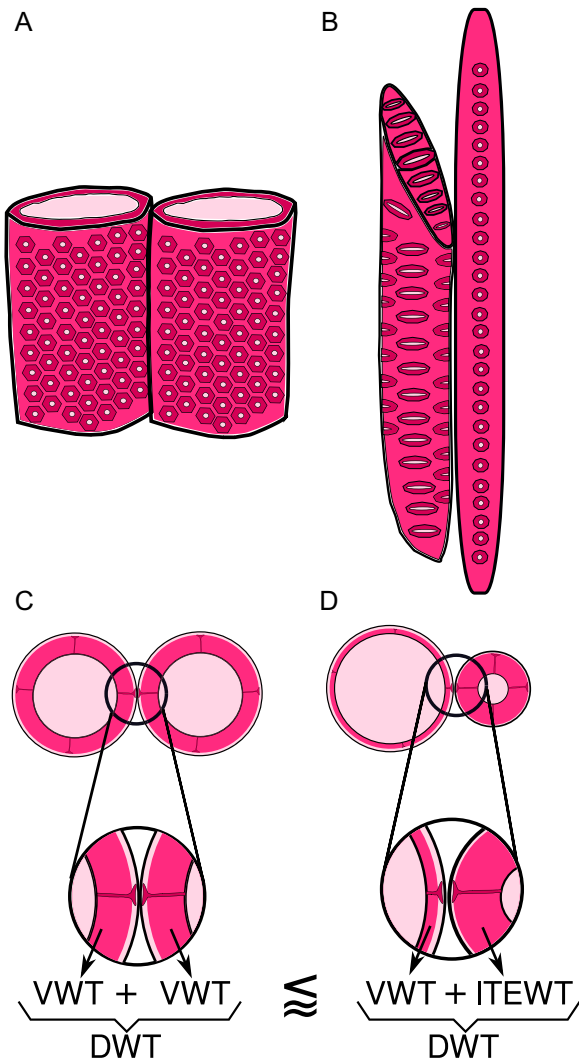
pressure, then we would expect less variation in the double wall thickness than the single; thin vessel walls and thick ITE walls, or thick vessel walls and thin ITE walls could both achieve the same double wall thickness. Consistent with this notion, despite the differences in vessel and ITE wall thickness between species with conductive and nonconductive ITEs, there was no significant difference between double wall thicknesses (Figures 3F, 5), which would be expected if the double wall, rather than the single wall, is the object of selection in the context of a given vessel diameter.

Biological signal in wall thickness–vessel diameter space below 90 μm diameter

The broad space of observed combinations of wall thickness and vessel diameters below 90 μm in vessel diameter (Figure 2) contained a great deal of biological signal, which we can only begin to explore here. We do so by examining the ecological preferences and habits of the 15 species with the most extreme values in the quadrants of this space, that is, species with very thick and very thin walls and narrow vessels, and very thick and very thin walls and wide vessels (Table 3; Appendices S2–S8). In some cases, we focus on the double wall and in others on the single, depending on which best highlights the anatomy–function relationship.

Thick walls, narrow vessels: species in saline drylands and herbaceous species with vessels embedded in a parenchyma background (upper left in Figure 4A)

The upper left quadrant of Figure 4A is occupied by species with very thick vessel walls and narrow vessels (Appendix S2). If thick vessel walls resist deformation of conduits and passage of embolisms, then species with very thick single-wall thicknesses and narrow vessels should be found in areas subject to high risk of embolism, and this is the case. Virtually all species in this quadrant are dryland plants. The thickest walls for a given diameter are plants that not only grow in dry areas, but saline ones as well, such as salt marshes and saline pans in interior drylands (Table 3). Finding that species of dry or saline areas, which are prone to highly negative soil water potentials, have thick walls and narrow vessels is therefore to be expected if this combination helps resist deformation under negative pressure (Hacke et al., 2001; Hacke and Sperry, 2001; Larter et al., 2015).

Among these species with exceptionally thick vessel walls and narrow vessels was the moist temperate herb *Helleborus viridis*, which represents a very different combination of hydraulically relevant traits. As a moist temperate herb, *H. viridis* was a distinct ecological exception among the dryland and even saline dryland species that are the other occupants of the quadrant (Appendix S2). As discussed above, if selection favors the double wall in resisting deformation, then in species that lack ITEs to which to transmit mechanical loads, then we

would expect exceptionally thick vessel walls for a given diameter because the single wall must resist the loads borne by the double walls in most other species. While some dryland species with relatively thick tracheid walls given diameter have been studied experimentally (e.g., Larter et al., 2015), the results here highlight saline dryland vessel-bearing species as likely being exceptionally resistant to embolism and meriting attention from functional studies (Olson et al., 2003), and herbaceous plants with thick vessel walls in a parenchyma background as a little-studied hydraulic syndrome.

Thin walls, narrow vessels: small plants of moist areas and deciduous dryland shrubs (lower left in Figure 4A)

The lower left quadrant of Figure 4A—exceptionally thin walls and narrow vessels—also is made up of at least two ecological types, both of which comprise small, shrubby plants (Table 3). One of these types is made up of shrubs or subshrubs of temperate, moist habitats. The other ecological type in this quadrant are chiefly shrubs or subshrubs of seasonally dry areas, either tropical or Mediterranean. Thin vessel walls on small plants of moist areas are not unexpected, because xylem pressures that are not highly negative plus small stature would not require resisting great mechanical loads. However, exceptionally thin walls for a given vessel diameter in dryland plants is conspicuous and highlights this combination as meriting attention. Some of the plants in this quadrant are soft-leaved species whose leaves wither in the dry season. Many soft-leaved deciduous or marcescent species have vasicentric or vascular tracheids (Carlquist, 1985), but species with these conductive ITEs tend to have high wood density and thick cell walls (Olson et al., 2020), unlike the species highlighted here. Instead, most of the species highlighted here lack vasicentric and vascular tracheids and likely have low wood density. For example, wood density data were available for *Buddleja stachyoides*, and it did indeed have lower wood density than species having thick wall, narrow vessels. Thus, deciduous subshrubs with very thin single and double walls merit attention as a distinctive hydraulic strategy.

Thick walls, wide vessels: *Ascarina* and the morphological cutoff between conductive and nonconductive imperforate tracheary elements (upper right in Figure 4A)

Of the 15 most extreme species in the quadrant at upper right in Figure 4A (Table 3; Appendix S2), species with wide vessels and exceptionally thick double walls, only two species had libriform fibers, a conspicuously low frequency because libriform fibers are the most common ITE type globally. In a survey of 641 angiosperm species, 59% had libriform fibers, 26% had true tracheids, and just 15% had fiber-tracheids (Olson et al., 2020). In the present data set, of the 841 species for which ITE type was given, 50% had

libriform fibers, 16% had true tracheids, and 34% had fiber-tracheids. Fully seven samples in this quadrant, representing five species, were from the genus *Ascarina* (Chloranthaceae). These species have grouped vessels and imperforate ITEs regarded as fiber-tracheids (Carlquist, 1990). The remainder of the species had either tracheids or fiber-tracheids. *Ascarina* emerges as conspicuous in this quadrant because, on morphological grounds, the imperforate tracheary elements in *Ascarina* appear to be (nonconductive) fiber-tracheids, but in our analysis, they behave more like (conductive) true tracheids. Morphologically, their pits, while distinctly bordered as in (conductive) true tracheids, are sparser in their occurrence on the ITE walls than on vessel lateral walls. This sparseness is not what would be expected in a conductive ITE. At the same time, vessels in *Ascarina* are grouped, which is not expected in the presence of true tracheids (Carlquist, 1984; Olson, 2020). Moreover, in at least two species of *Ascarina* (*A. rubricaulis* and *A. diffusa*), the ITEs actually bear septa, that is, primary walls traversing the ITE lumen, dividing it into two or more ostensibly living compartments. Septa seem certain to diagnose nonconductive ITEs (Sano et al., 2011). It is not known whether there is a sharp division between conductive and nonconductive ITEs or whether there is a gradient, with some species having fiber-tracheids that conduct, albeit less than paradigm true tracheids. Because most of the species in this quadrant possess the signs of having true tracheids, the fact that *Ascarina* groups with them calls into question whether or not the "fiber-tracheids" in these species are not in fact (conductive) true tracheids. This result highlights this genus as a suitable model for exploring the morphological correlates of conductive status in ITEs (in the spirit of Sano et al., 2011). The conductive or nonconductive status of the species, with both septate and nonseptate ITEs, could be examined. As part of this effort, quantifying the dimensions and sparseness of pits, and intactness of membranes, would shed light on the quantitative morphological thresholds between conductive and nonconductive ITEs, and the relationship between vessel grouping and ITE function. Such studies will go a long way toward determining whether the "fiber tracheid" category is morphologically and functionally distinct from tracheids and libriform fibers or whether it is an arbitrary one, in addition to identifying the morphological correlates of conductive status in ITEs.

Thin walls, wide vessels: evergreen pioneer species (lower right in Figure 4A)

Like the upper and lower left quadrants, the lower right quadrant of Figure 4A also revealed two highly divergent ecological strategies. These two strategies were evident in both analyses of the single- and the double-wall–vessel diameter relationship (Appendix S2). Not surprisingly, several of the occupants of the thin single vessel wall–wide vessels quadrant were species of mostly cool, moist habitats with presumably xylem pressures that are not highly negative year-round or at least during the growing season. Finding relatively thin vessel walls in moist, often tropical highland, forest species is consistent with the notion that these habitats experience little water deficit during the growing season. Surprising, however, was the finding of evergreen species of dry habitats in the thin vessel wall–vessel diameter quadrant. These included *Eriodictyon californicum* and *Wigandia urens* (Boraginaceae) and *Nicotiana glauca* (Solanaceae), all evergreen pioneer species that establish in open, dry areas. Even with stomata closed, leaves continue to lose water across the cuticle, especially under hot, dry conditions (Duursma et al., 2019; Aparecido et al., 2020), making the evergreen habit of the species in the lower right quadrant of Figure 4A all the more conspicuous. It is not clear how these species maintain their leaves even through drought with their wide vessels and exceptionally thin cell walls, which are presumably relatively vulnerable to embolism. All three of these species often persist evergreen on very dry microsites (Appendix S9). Our results thus highlight the combination of wide vessels, thin vessel and ITE walls, and an evergreen habit in warm, dry pioneer species as a distinctive and little-studied hydraulic strategy.

CONCLUSIONS

Our results suggest that while selection can favor a very wide array of wall thickness–vessel diameter combinations below the 90 μm threshold, above this threshold variants with walls that are "too thick" are uncommon, likely because of excessive carbon cost in most situations, and those with walls that are "too thin" are probably eliminated because they do not resist deformation. Our results also provide evidence that both the single vessel wall as well as the vessel+adjacent cell wall thickness can be shaped by selection. In addition, our approach highlights the value of comparative data in identifying the range of plant hydraulic syndromes that require detailed study (cf. Janssen et al., 2020). Our analyses highlight plants of saline drylands, small plants with vessels in a parenchyma background, deciduous dryland shrubs with low wood density, cloud forest true tracheid- and fiber-tracheid-bearing species with scalariform perforation plates, and evergreen dryland pioneers with low wood density as little-studied hydraulic syndromes. We can also mention water-storing trees (bottle trees, giant tree cacti, and euphorbias, etc.), species with successive cambia, and those with conductive ITEs, as very common but little-examined hydraulic syndromes. All of these syndromes mentioned probably span more species and geographical area than ring-porous species, which, despite being restricted to few species of the north temperate zone, are routinely examined in physiological studies. These little-studied syndromes require attention in the effort to construct an understanding of xylem structure–function relationships that parallels the true diversity of xylem anatomy across the vascular plants.

DATA AVAILABILITY STATEMENT

The data set is available at the TRY File Archive (https://www.try-db.org/TryWeb/Data.php#82; DOI: 10.17871/TRY.82), and the code used for the analyses is available at https://github.com/echeverria-alberto/WallThickness-VesselDiameter.

ORCID

Alberto Echeverría http://orcid.org/0000-0001-7940-1592
Emilio Petrone-Mendoza http://orcid.org/0000-0003-2130-3927
Mark E. Olson http://orcid.org/0000-0003-3715-4567

REFERENCES

Aparecido, L. M. T., S. Woo, C. Suazo, K. R. Hultine, and B. Blonder. 2020. High water use in desert plants exposed to extreme heat. *Ecology Letters* 23: 1189–1200.

Baas, P., E. Werker, and A. Fahn. 1983. Some ecological trends in vessel characters. *IAWA Journal* 4: 141–159.

Blackman, C. J., S. M. Gleason, A. M. Cook, Y. Chang, C. A. Laws, and M. Westoby. 2018. The links between leaf hydraulic vulnerability to drought and key aspects of leaf venation and xylem anatomy among 26 Australian woody angiosperms from contrasting climates. *Annals of Botany* 122: 59–67.

Bouda, M., C. W. Windt, A. J. McElrone, and C. R. Brodersen. 2019. In vivo pressure gradient heterogeneity increases flow contribution of small diameter vessels in grapevine. *Nature Communications* 10: 5645.

Bryant, C., N. R. Wheeler, F. Rubel, and R. H. French. 2017. kgc: Koeppen-Geiger climatic zones. R package version 1.0.0.2. Website: https://CRAN.R-project.org/package=kgc

Carlquist, S. 1984. Vessel grouping in dicotyledon wood: significance and relationship to imperforate tracheary elements. *Aliso* 10: 505–525.

Carlquist, S. 1985. Vasicentric tracheids as a drought survival mechanism in the woody flora of southern California and similar regions; review of vasicentric tracheids. *Aliso* 11: 37–68.

Carlquist, S. 1986. Terminology of imperforate tracheary elements. *IAWA Journal* 7: 75–81.

Carlquist, S. 1990. Wood anatomy of *Ascarina* (Chloranthaceae) and the tracheid-vessel element transition. *Aliso* 12: 667–684.

Carlquist, S. 1995. Wood and bark anatomy of Ranunculaceae (Including *Hydrastis*) and Glaucidiaceae. *Aliso* 14: 65–84.

Carlquist, S. 2000. Wood and stem anatomy of phytolaccoid and rivinoid Phytolaccaceae (Caryophyllales): ecology, systematics, nature of successive cambia. *Aliso* 19: 13–29.

Carlquist, S. 2001. Comparative wood anatomy, ed 2. Springer, Berlin, Germany.

Carlquist, S. 2017. What the Penaeaceae alliance (Myrtales) tells us about the nature of vestured pits in xylem. *Brittonia* 69: 276–294.

Cayuela, L., I. Macarro, A. Stein, and J. Oksanen. 2021. Taxonstand: Taxonomic standardization of plant species names. R package version 2.4 Website https://CRAN.R-project.org/package=Taxonstand

Chaffey, N., E. Cholewa, S. Regan, and B. Sundberg. 2002. Secondary xylem development in *Arabidopsis*: a model for wood formation. *Physiologia Plantarum* 114: 594–600.

Chase, M. W., M. J. M. Christenhusz, M. F. Fay, J. W. Byng, W. S. Judd, D. E. Soltis, D. J. Maberley, et al. 2016. An update of the Angiosperm Phylogeny Group classification for the orders and families of flowering plants: APG IV. *Botanical Journal of the Linnean Society* 181: 1–20.

Chen, Z., S. Zhu, Y. Zhang, J. Luan, S. Li, P. Sun, X. Wan, and S. Liu. 2020. Tradeoff between storage capacity and embolism resistance in the xylem of temperate broadleaf tree species. *Tree Physiology* 40: 1029–1042.

Cochard, H., S. T. Barigah, M. Kleinhentz, and A. Eshel. 2008. Is xylem cavitation resistance a relevant criterion for screening drought resistance among *Prunus* species? *Journal of Plant Physiology* 165: 976–982.

Donaldson, L. A. 2002. Abnormal lignin distribution in wood from severely drought stressed *Pinus radiata* trees. *IAWA Journal* 23: 161–178.

Duursma, R. A., C. J. Blackman, R. Lopéz, N. K. Martin-StPaul, H. Cochard, and B. E. Medlyn. 2019. On the minimum leaf conductance: its role in models of plant water use, and ecological and environmental controls. *New Phytologist* 221: 693–705.

Fajardo, A. 2022. Wood density relates negatively to maximum plant height across major angiosperm and gymnosperm orders. *American Journal of Botany* 109: 250–258.

Frost, F. H. 1930. Specialization in secondary xylem of dicotyledons. II. Evolution of end wall of vessel segment. *Botanical Gazette* 90: 198–212.

Guet, J., R. Fichot, C. Lédée, F. Laurans, H. Cochard, S. Delzon, C. Bastien, and F. Brignolas. 2015. Stem xylem resistance to cavitation is related to xylem structure but not to growth and water-use efficiency at the within-population level in *Populus nigra* L. *Journal of Experimental Botany* 66: 4643–4652.

Hacke, U. G., and J. S. Sperry. 2001. Functional and ecological xylem anatomy. *Perspectives in Plant Ecology, Evolution and Systematics* 4: 97–115.

Hacke, U. G., J. S. Sperry, W. T. Pockman, S. D. Davis, and K. A. McCulloh. 2001. Trends in wood density and structure are linked to prevention of xylem implosion by negative pressure. *Oecologia* 126: 457–461.

Hijmans, R. J., J. van Etten, M. Sumner, J. Cheng, D. Baston, A. Bevan, Roger Bivand, et al. 2021. raster: Geographic data analysis and modeling. R package version 3.5-15. Website: https://CRAN.R-project.org/package=raster

Hölttä, T., Mencuccini M. & Nikinmaa E. (2011) A carbon cost-gain model explains the observed patterns of xylem safety and efficiency: a carbon gain–cost model for xylem structure. *Plant, Cell & Environment* 34: 1819–1834.

Jacobsen, A. L., L. Agenbag, K. J. Esler, R. B. Pratt, F. W. Ewers, and S. D. Davis. 2007. Xylem density, biomechanics and anatomical traits correlate with water stress in 17 evergreen shrub species of the Mediterranean-type climate region of South Africa. *Journal of Ecology* 95: 171–183.

Jacobsen, A. L., F. W. Ewers, R. B. Pratt, W. A. Paddock, and S. D. Davis. 2005. Do xylem fibers affect vessel cavitation resistance? *Plant Physiology* 139: 546–556.

Janssen, T. A. J., T. Hölttä, K. Fleischer, K. Naudts, and H. Dolman. 2020. Wood allocation trade-offs between fiber wall, fiber lumen, and axial

parenchyma drive drought resistance in neotropical trees. *Plant, Cell & Environment* 43: 965–980.

Kaack, L., M. Weber, E. Isasa, Z. Karimi, S. Li, L. Pereira, C. L. Trabi, et al. 2021. Pore constrictions in intervessel pit membranes provide a mechanistic explanation for xylem embolism resistance in angiosperms. *New Phytologist* 230: 1829–1843.

Karam, G. N. 2005. Biomechanical model of the xylem vessels in vascular plants. *Annals of Botany* 95: 1179–1186.

Kattge, J., G. Bönisch, S. Díaz, S. Lavorel, I. C. Prentice, P. Leadley, S. Tautenhahn, et al. 2020. TRY plant trait database—enhanced coverage and open access. *Global Change Biology* 26: 119–188.

Koçillari, L., M. E. Olson, S. Suweis, R. P. Rocha, A. Lovison, F. Cardin, T. E. Dawson, et al. 2021. The Widened Pipe Model of plant hydraulic evolution. *Proceedings of the National Academy of Sciences, USA* 118: e2100314118.

Kottek, M., J. Grieser, C. Beck, B. Rudolf, and F. Rubel. 2006. World map of the Köppen-Geiger climate classification updated. *Meteorologische Zeitschrift* 15: 259–263.

Larson, P. R. 1994. Vascular cambium: development and structure. Springer-Verlag, Berlin, Germany.

Larter, M., T. J. Brodribb, S. Pfautsch, R. Burlett, H. Cochard, and S. Delzon. 2015. Extreme aridity pushes trees to their physical limits. *Plant Physiology* 168: 804–807.

Lens, F., J. S. Sperry, M. A. Christman, B. Choat, D. Rabaey, and S. Jansen. 2011. Testing hypotheses that link wood anatomy to cavitation resistance and hydraulic conductivity in the genus *Acer*. *New Phytologist* 190: 709–723.

Levionnois, S., S. Jansen, R. T. Wandji, J. Beauchêne, C. Ziegler, S. Coste, C. Stahl, et al. 2021. Linking drought-induced xylem embolism resistance to wood anatomical traits in Neotropical trees. *New Phytologist* 229: 1453–1466.

Li, S., F. Lens, S. Espino, Z. Karimi, M. Klepsch, H. J. Schenk, M. Schmitt, et al. 2016. Intervessel pit membrane thickness as a key determinant of embolism resistance in angiosperm xylem. *IAWA Journal* 37: 152–171.

Maitner, B. S., B. Boyle, N. Casler, R. Condit, J. Donoghue, S. M. Durán, D. Guaderrama, et al. 2018. The BIEN R package: a tool to access the Botanical Information and Ecology Network (BIEN) database. *Methods in Ecology and Evolution* 9: 373–379.

Mencuccini, M., T. Hölttä, G. Petit, and F. Magnani. 2007. Sanio's laws revisited. *Size-dependent changes in the xylem architecture of trees. Ecology Letters* 10: 1084–1093.

Nardini, A., G. Pedà, and N. L. Rocca. 2012. Trade-offs between leaf hydraulic capacity and drought vulnerability: morpho-anatomical bases, carbon costs and ecological consequences. *New Phytologist* 196: 788–798.

Olson, M. E. 2012. The developmental renaissance in adaptationism. *Trends in Ecology & Evolution* 27: 278–287.

Olson, M. E. 2019. Overcoming the constraint–adaptation dichotomy: long live the constraint–adaptation dichotomy. *In* G. Fusco [ed.], Perspectives on evolutionary and developmental biology, 78–94. University of Padova Press, Padova, Italy.

Olson, M. E. 2020. From Carlquist's ecological wood anatomy to Carlquist's Law: Why comparative anatomy is crucial for functional xylem biology. *American Journal of Botany* 107: 1328–1341.

Olson, M. E., T. Anfodillo, S. M. Gleason, and K. A. McCulloh. 2021. Tip-to-base xylem conduit widening as an adaptation: causes, consequences, and empirical priorities. *New Phytologist* 229: 1877–1893.

Olson, M. E., J. F. Gaskin, and F. Ghahremani-Nejad. 2003. Stem anatomy is congruent with molecular phylogenies placing *Hypericopsis persica* in *Frankenia* (Frankeniaceae): comments on vasicentric tracheids. *Taxon* 52: 525–532.

Olson, M. E., J. A. Rosell, C. Martínez-Pérez, C. León-Gómez, A. Fajardo, S. Isnard, M. A. Cervantes-Alcayde, et al. 2020. Xylem vessel diameter–shoot length scaling: ecological significance of porosity types and other traits. *Ecological Monographs* 90: e01410.

Pebesma, E., R. Bivand, B. Rowlingson, V. Gomez-Rubio, R. Hijmans, M. Sumner, D. MacQueen, et al. 2021. sp: classes and methods for spatial data. R package version 1.2-1. Website: https://CRAN.R-project.org/package=sp

Pfautsch, S., M. J. Aspinwall, J. E. Drake, L. Chacon-Doria, R. J. A. Langelaan, D. T. Tissue, M. G. Tjoelker, et al. 2018. Traits and trade-offs in whole-tree hydraulic architecture along the vertical axis of *Eucalyptus grandis*. *Annals of Botany* 121: 129–141.

Pittermann, J., J. S. Sperry, J. K. Wheeler, U. G. Hacke, and E. H. Sikkema. 2006. Mechanical reinforcement of tracheids compromises the hydraulic efficiency of conifer xylem. *Plant, Cell and Environment* 29: 1618–1628.

Pratt, R. B., A. L. Jacobsen, F. W. Ewers, and S. D. Davis. 2007. Relationships among xylem transport, biomechanics and storage in stems and roots of nine Rhamnaceae species of the California chaparral. *New Phytologist* 174: 787–798.

Ranocha, P., N. Denancé, R. Vanholme, A. Freydier, Y. Martinez, L. Hoffmann, L. Köhler, et al. 2010. Walls are thin 1 (WAT1), an *Arabidopsis* homolog of *Medicago truncatula* NODULIN21, is a tonoplast-localized protein required for secondary wall formation in fibers: Tonoplastic WAT1 and secondary wall formation. *Plant Journal* 63: 469–483.

Rosell, J. A., M. E. Olson, R. Aguirre-Hernández, and S. Carlquist. 2007. Logistic regression in comparative wood anatomy: tracheid types, wood anatomical terminology, and new inferences from the Carlquist and Hoekman southern Californian data set. *Botanical Journal of the Linnean Society* 154: 331–351.

Sano, Y., H. Morris, H. Shimada, L. P. Ronse De Craene, and S. Jansen. 2011. Anatomical features associated with water transport in imperforate tracheary elements of vessel-bearing angiosperms. *Annals of Botany* 107: 953–964.

Scholz, A., M. Klepsch, Z. Karimi, and S. Jansen. 2013a. How to quantify conduits in wood? *Frontiers in Plant Science* 4: 56.

Scholz, A., D. Rabaey, A. Stein, H. Cochard, E. Smets, and S. Jansen. 2013b. The evolution and function of vessel and pit characters with respect to cavitation resistance across 10 *Prunus* species. *Tree Physiology* 33: 684–694.

Sorz, J., and P. Hietz. 2006. Gas diffusion through wood: implications for oxygen supply. *Trees* 20: 34–41.

Spatz, H.-C., and K. J. Niklas. 2013. Modes of failure in tubular plant organs. *American Journal of Botany* 100: 332–336.

Steppe, K., F. Sterck, and A. Deslauriers. 2015. Diel growth dynamics in tree stems: linking anatomy and ecophysiology. *Trends in Plant Science* 20: 335–343.

Sterck, F. J., J. Martínez-Vilalta, M. Mencuccini, H. Cochard, P. Gerrits, R. Zweifel, A. Herrero, et al. 2012. Understanding trait interactions and their impacts on growth in Scots pine branches across Europe: functional branch trait coordination. *Functional Ecology* 26: 541–549.

Thonglim, A., S. Delzon, M. Larter, O. Karami, A. Rahimi, R. Offringa, J. J. B. Keurentjes, et al. 2020. Intervessel pit membrane thickness best explains variation in embolism resistance amongst stems of *Arabidopsis thaliana* accessions. *Annals of Botany* 128: 171–182.

Turner, S. R., and C. R. Somerville. 1997. Collapsed xylem phenotype of *Arabidopsis* identifies mutants deficient in cellulose deposition in the secondary cell wall. *Plant Cell* 9: 689–701.

Venturas, M. D., J. S. Sperry, and U. G. Hacke. 2017. Plant xylem hydraulics: What we understand, current research, and future challenges: plant xylem hydraulics. *Journal of Integrative Plant Biology* 59: 356–389.

Wheeler, E. A., P. Baas, and P. E. Gasson (eds). 1989. IAWA list of microscopic features for hardwood identification. *IAWA Journal* 10: 219–332.

SUPPORTING INFORMATION

Additional supporting information can be found online in the Supporting Information section at the end of this article.

Appendix S1. Relationship between vessel wall thickness and vessel diameter above the 90 μm threshold.

Appendix S2. Species with extreme combinations of vessel wall thickness and vessel diameter below the 90 μm threshold (corresponding to the quadrants in Figure 4A).

Appendix S3. Species with extreme combinations of double wall (vessel+ITE) thickness and vessel diameter, below the 90 µm threshold (corresponding to the quadrants in Figure 4A).

Appendix S4. Whittaker plot showing climate space covered by the sampled species.

Appendix S5. Distribution of Köppen climates across the entire data set and in the four extremes in Appendices S2 and S3.

Appendix S6. Distribution of (A) growth form woodiness and (B) phenology across the vessel diameter–vessel wall thickness relationship.

Appendix S7. Mean wood density of species from the extreme combinations of vessel wall thickness and vessel diameter.

Appendix S8. Wood density in the Carlquist data set.

Appendix S9. Evergreen pioneers in dry areas with thin vessel and vessel-ITE walls and wide vessels.